[Article] www.whxb.pku.edu.cn

阴离子表面活性剂在水/正烷烃界面的分子动力学模拟

肖红艳[1,*] 甄 珍[1] 孙焕泉[2] 曹绪龙[2] 李振泉[2]
宋新旺[2] 崔晓红[2] 刘新厚[1,*]

([1]中国科学院理化技术研究所, 光化学转换与功能材料重点实验室, 北京 100190;
[2]中石化胜利油田分公司地质科学研究院, 山东 东营 257001)

摘要: 利用分子动力学模拟方法研究了阴离子表面活性剂在水/正烷烃(壬烷, 癸烷和十一碳烷)界面的结构和动力学特点. 十六烷基苯磺酸钠作为研究对象, 其中苯磺酸基团在十六碳烷的第 4 号碳原子上, 记作 4-C16. 分析了不同油相和特定盐度条件下正烷烃-表面活性剂-水体系的界面特点(如密度剖面图、界面张力和径向分布函数). 模拟结果表明平衡模型体系展现了一个很好的水/正烷烃界面. 当加氯化钠到水溶液中, 正烷烃-表面活性剂-水体系的界面张力有微小的变化, 有趣的是表面活性剂二面角的反式结构分数的变化联系着界面张力的微小变化. 可见, 表面活性剂在界面处的结构对降低界面张力起到重要的作用. 此外, 还发现表面活性剂的极性头与钠离子和水分子存在较强的相互作用.

关键词: 分子动力学; 水/正烷烃界面; 阴离子表面活性剂; 界面张力; 反式结构分数
中图分类号: O641; O647

Molecular Dynamics Simulation of Anionic Surfactant at the Water/*n*-Alkane Interface

XIAO Hong-Yan[1,*] ZHEN Zhen[1] SUN Huan-Quan[2] CAO Xu-Long[2] LI Zhen-Quan[2]
SONG Xin-Wang[2] CUI Xiao-Hong[2] LIU Xin-Hou[1,*]

([1]*Key Laboratory of Photochemical Conversion and Optoelectronic Materials, Technical Institute of Physics and Chemistry, Chinese Academy of Sciences, Beijing 100190, P. R. China*; [2]*Institute of Geological Science, Shengli Oilfield Ltd. Co., Dongying 257001, Shandong Province, P. R. China*)

Abstract: The structural and dynamic properties of anionic surfactant at the water/*n*-alkane (nonane, decane, and undecane) interface were investigated by the molecular dynamics simulation. The model anionic surfactant contained a benzene sulfonate group attached to the 4th carbon in the hexadecane backbone and was denoted as 4-C16. We analyzed the interfacial properties (density profile, interfacial tension, and radial distribution function) of the *n*-alkane-surfactant-water systems in different oil phases and under special inorganic salinity conditions. The simulation results indicate that a well-defined interface exists between the *n*-alkane and water phases in the equilibrated model systems. The interfacial tensions of the *n*-alkane-surfactant-water systems show little change when sodium chloride is added to the solutions. We find that a change in the *trans*-form fraction of the dihedral in 4-C16 is related to a subtle change in the interfacial tension at the water/*n*-alkane interface. Clearly, the structure of the surfactant at the interface plays an important role in reducing the interfacial tension. In addition, we also find that the polar head group of the surfactant molecules with sodium ions and water molecules undergo stronger interactions.

Key Words: Molecular dynamics; Water/*n*-alkane interface; Anionic surfactant; Interfacial tension; *trans*-form fraction

Received: September 29, 2009; Revised: December 1, 2009; Published on Web: December 23, 2009.
*Corresponding authors. Email: hyxiao@mail.ipc.ac.cn, zhenz@mail.ipc.ac.cn; Tel: +86-10-82543529
Ⓒ Editorial office of Acta Physico-Chimica Sinica

Surfactant flooding is an important form in the enhanced crude oil recovery. The main function of the surfactant is to reduce the interfacial tension between oil and water to an ultra-low value ($<10^{-3}$ mN·m^{-1}). Therefore, it is necessary to understand the underlying principles governing the interfacial properties in order to design and synthesize the optimizing surfactants.

Long linear alkylbenzene sulfonate is a kind of very popular surfactants which are widely used in industry and daily life. Many studies have been done from the point of the experimental and theoretical views. Baumgartner[1] synthesized a series of dodecylbenzene sulfonate sodium isomers and investigated the branching of the hydrophobic alkyl chain effect on their properties. Doe *et al*.[2–3] studied the alkane preference of linear alkylbenzene sulfonate surfactants in alkane/aqueous system and proposed the concept of the minimum alkane carbon number (n_{min}). Yang *et al*.[4] reported the interfacial behavior of a series of hexadecylbenzene sulfonate isomers and discussed the relationship between electrolyte concentration and interfacial tension minima. The branched alkylbenzene sulfonates and their properties of interface and solutions were investigated[5]. As for the theoretical aspect, molecular simulations have become an important tool for the study of the complex interfacial systems, because it could provide the dynamical, thermodynamical, and structural properties of the interfacial systems at the molecular level, which are not easy to be obtained from the experiments. For examples, Li *et al*.[6–7] used the dissipative particle dynamics method to simulate the absorption of sodium dodecylbenzene sulfonate (SDBS) and sodium oleate (OAS) at the oil/water interface. Their investigations showed that it was beneficial to decrease interfacial tension if the hydrophobic chains of surfactant and the oil had the similar structure; in addition, the accession of inorganic salts caused the surfactant molecules to form more compact and ordered arrangement and helped to decrease the interfacial tension. Goddard *et al*.[8] investigated the effect of molecular architecture of alkyl benzene sulfonate at the water/decane interface. They suggested that the interfacial tension was related to the miscibility of the alkyl tail of surfactant with decane. While Yang *et al*.[4] considered that the interfacial tension depended on the status of the surfactant molecules adsorbing on the interface, especially the properties of the outermost atoms or groups at the interface region.

The 4-C16 anion surfactant with a benzene sulfonate group attached to the 4th carbon in hexadecane backbone, is a representative of long linear alkylbenzene sulfonates. In this paper, we will take it as an example to investigate the interfacial properties of the surfactant at the water/*n*-alkane interface under the different oil phases and the special inorganic salinity conditions in detail using molecular dynamics (MD) method, in order to gain an insight into the interfacial characteristics of long linear alkylbenzene sulfonates at the water/oil interface.

1 Model and simulation methods

Geometry structure of the 4-C16 surfactant was optimized using the B3LYP/6-31+g(*d*) method, Gaussian 03 package[9] and then the optimized structure was used to build the modeling system. See Fig.1 for the schematic diagram and atom number of the surfactant. The molecular packing program Packmol[10] was used to build two opposite surfactant monolayers at the *n*-alkane/water/*n*-alkane interfaces, as shown in Fig.2. The two monolayers and the water phase were placed in the middle of this box, with the normal to the monolayers pointing in the *z*-direction. *n*-alkane (nonane, decane, and undecane) molecules were placed on both sides of the monolayers to give the oil phase density based on the corresponding experimental values[11]. The density of water in the initial model was set to 0.997×10^3 kg·m^{-3} [12]. An initial periodic box was depicted with a size of 5.0 nm×5.0 nm×14.0 nm (*x*- , *y*-, and *z*- directions, respectively). The number of molecules in the simulation systems is listed in Table 1. In order to make the system neutrality, sodium ions were added at the water/*n*-alkane interface. In addition, considering the salt effect, the salt was included by randomly adding 15 Na^+ (besides the Na^+ ions from the surfactant molecules) and 15 Cl^- particles into the water solution (namely 0.17 mol·L^{-1} NaCl solution). Six systems including the surfactants at the water(-NaCl)/nonane, water(-NaCl)/decane, and water(-NaCl)/undecane interfaces were studied.

In this simulation, periodic boundary condition was applied in all three spatial dimensions. *n*-alkane was described using the united atom model[13] and water using the SPC model[14]. For the 4-C16 surfactant, the benzene sulfonate part was described by the explicit all-atom model, and the alkyl tail part was described by the same united atom model used for *n*-alkane[13]. The topology file of the 4-C16 surfactant was produced by the Prodrg program[15]. The energy of a molecular system was described by the simple potential energy functions comprising the bond stretching, bond

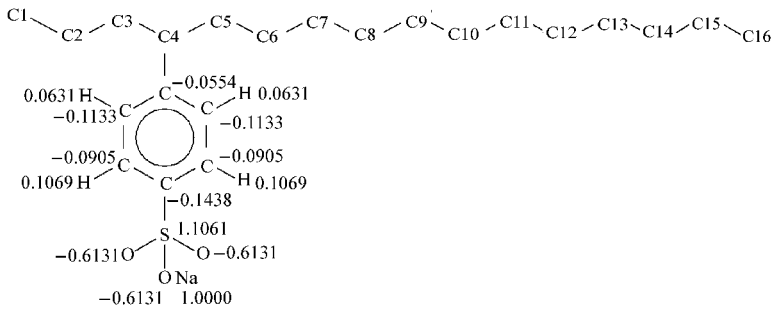

Fig.1 Structure and partial charges (*e*) of the 4-C16 surfactant

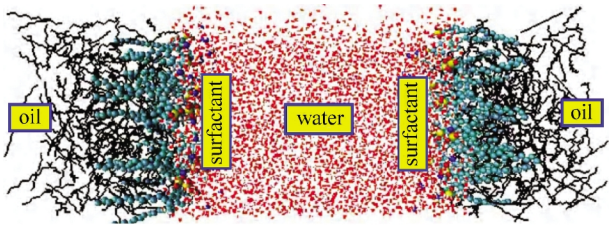

Fig.2 Simulated configuration of the water/*n*-alkane interface in the presence of a surfactant monolayer

Table 1 Number (*N*) of molecules comprised simulation systems

N_{water}	$N_{surfactant}$	N_{nonane}	N_{decane}	$N_{undecane}$
5016	50	506	462	428

angle bending, torsional, Lennard-Jones, and electrostatic interactions. For the bond stretching and bond angle bending interactions, the harmonic potential was used; for the dihedrals of $CH_2CH_2CH_2CH_2$ and $CH_3CH_2CH_2CH_2$, the Ryckaert-Bellemans potential[16] was used (which gives better statistics on the *trans*/*gauche* behavior). All MD simulations were performed with Gromacs 4.0 package[17–20]. The force field parameters used to calculate the intra- and inter-molecular interactions were from ffG53a6 force field, and the partial charge′s parameters were from Ref.[8] (see Fig.1). The Lennard-Jones potential parameters for the van der Waals interaction of heterogeneous atomic pairs were calculated from the geometric mean of parameters of each atom. Considering the sensitivity of surface properties to the van der Waals parameters, van Buuren *et al.*[13] did a systematic research on the decane/water interface and provided the modified van der Waals parameters of ε_{O-CH_3}=0.849 kJ·mol^{-1}, ε_{O-CH_2}=0.706 kJ·mol^{-1}, and σ_{O-C}=0.344 nm. Therefore, we used the modified parameters during the simulations.

To remove the initial strain of system, energy minimization was performed on the initial configuration. Then, 100 ps constraint dynamics simulations were carried out, in which the surfactant monolayers were restrained and the initial velocities were generated based on Maxwellian distribution at 300 K. The following 200 ps NVT (canonical ensemble) and 400 ps NPT (isothermal-isobaric ensemble) MD simulations were sequentially carried out to equilibrate the system. To obtain good statistics, two independent samples of 2 ns NPT MD simulation for each water(-NaCl)/*n*-alkane case were performed. All the covalent bond lengths were constrained by LINCS algorithm[21] and a time step of 2.0 fs was used in all simulations. The temperature was controlled using the Nose-Hoover thermostat[22–24] with relaxation time of 0.1 ps. The Parrinello-Rahman pressure scaling[25–26] was performed isotropically by coupling to a pressure bath of 10^5 Pa (time constant: 0.5 ps). A twin-range cutoff for non-bonded forces of 0.9/1.4 nm was used; the pair list and forces for the range between 0.9 and 1.4 nm were updated every 10 steps.

2 Results and discussion

2.1 Liquid density profile

Fig.3 shows the density profiles of each system along the *z*-axis direction of the simulation box, which were obtained by calculating the density in 100 slabs parallel to the *xy* plane. From the density profiles, it is clear that every system consists of two phases (invariant density with *z*) with two well-defined interfaces (varying density with *z*). It should be noticed that the densities of each phase in the *n*-alkane-surfactant-water system (0.709×10^3 kg·m^{-3} for nonane, 0.726×10^3 kg·m^{-3} for decane, 0.737×10^3 kg·m^{-3} for undecane, and 0.982×10^3 kg·m^{-3} for water) agree well with those of the pure bulk phase (0.718×10^3 kg·m^{-3} for nonane[11], 0.730×10^3 kg·m^{-3} for decane[11], 0.740×10^3 kg·m^{-3} for undecane[11], and 0.997×10^3 kg·m^{-3} for water[12]). It indicates that the size of our simulation is large enough to study a realistic interface between two bulk phases. Besides, it is found that most of the sodium ions stay at the interval between the water and the surfactant monolayer, and a few ions are dispersed into the water solution. As shown in Fig.3, the similarities between Fig.3(a) and 3(d), 3(b) and 3(e), 3(c) and 3(f) mean that the influence of salt on the density is very little, due to the lower salt concentrations.

2.2 Interfacial tension

The interfacial tension (γ) is defined, when the interface is perpendicular to the *z* axis[27–28], as

$$\gamma(t)=\frac{1}{2}\int_0^{L_z}\left\{p_{zz}(z,t)-\frac{p_{xx}(z,t)+p_{yy}(z,t)}{2}\right\}\mathrm{d}z$$
$$=\frac{L_z}{2}\left\{p_{zz}(t)-\frac{p_{xx}(t)+p_{yy}(t)}{2}\right\} \quad (1)$$

where p_{zz} is the normal pressure, p_{xx} and p_{yy} are the tangential pressures with respect to the planar interface.

According to the Eq.(1), we calculated the interfacial tensions of the 4-C16 surfactant at the water/*n*-alkane interface. The results are listed in Table 2. As shown in Table 2, the water/decane interface has the lowest interfacial tension. Qualitatively, it agrees with the experimental observation[5] that the interfacial tension of the 4-C16 surfactant at the water/*n*-alkane interface varies as the alkyl chain length changes and the water/decane interface has the lowest interfacial tension. When NaCl is added to the solution, the interfacial tensions have a little change. Compared with the interfacial tension of the 4-C16 surfactant in the water/*n*-alkane, the interfacial tension decreases in the water-NaCl/nonane, increases in the water-NaCl/decane, and hardly changes in the water-NaCl/undecane. Similar to our simulation, the little variation of the interfacial tension has also been observed in the mixed system of 0.17 mol·L^{-1} NaCl solution and *n*-alkane experimentally[5]. Therefore, we will further analyze the interfacial tension change in the following sections.

First, we calculated the alkyl tail length of *n*-alkane and surfactant. The effective alkyl tail length of surfactant has been defined as $r_{effective}=r_{long}-r_{short}$ by Jang and co-workers (see Fig.11 in Ref.[8]). For the 4-C16 surfactant, r_{long} denotes the tail length from C4 to C16, and r_{short} denotes the tail length from C4 to C1 (see Fig.1). As shown in Table 3, the calculated $r_{effective}$ of 4-C16 is similar to the length of nonane (r_{nonane}=(0.859±0.014) nm), and shorter than the length of decane (r_{decane}=(0.951±0.019) nm). It is not comprehensive to explain the interfacial tension change in

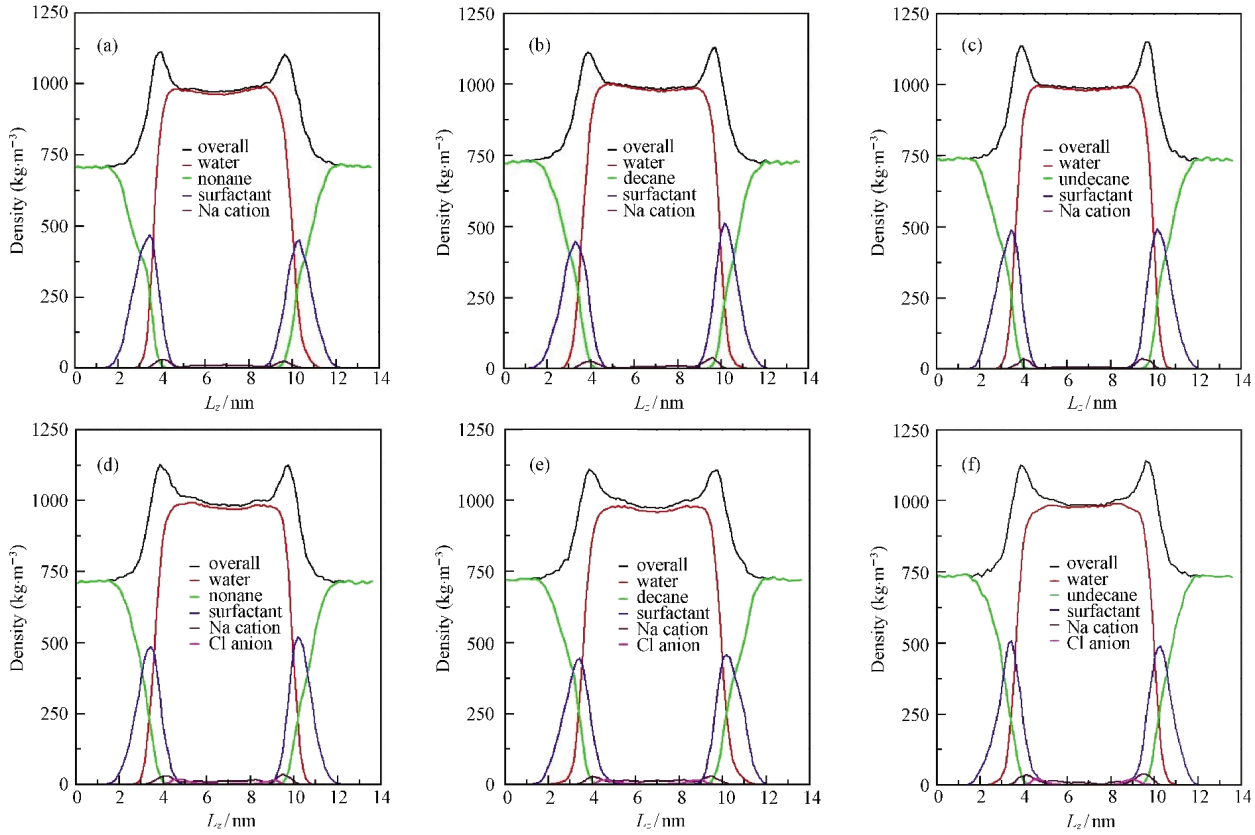

Fig.3 Density profiles along the *z*-axis direction of the simulation box

(a) water/nonane, (b) water/decane, (c) water/undecane, (d) water-NaCl/nonane, (e) water-NaCl/decane, (f) water-NaCl/undecane; L_z is the box length along the *z*-axis direction.

Table 2 Calculated interfacial tensions of the 4-C16 surfactant at the water/*n*-alkane interface

n-alkane	γ(water/*n*-alkane)/(mN·m^{-1})	γ(water-NaCl/*n*-alkane)/(mN·m^{-1})
nonane	33.14±0.62	31.41±0.05
decane	27.42±1.53	31.04±0.32
undecane	31.10±3.31	31.08±3.41

terms of the miscibility of the alkyl tail of the 4-C16 surfactant with decane as described in Ref.[8]. A point of view[6–7] is that the similar structures between the hydrophobic chains of surfactant and the oil will reduce the interfacial tension. However, the hydrophobic chain of surfactant is usually the linear chain. The surfactant with the branching structure will affect the miscibility with the oil phase. As the 4-C16 surfactant has two alkyl tail chains, the interfacial tension has the lowest value at the water/decane interface, while the lengths of $r_{\text{effective}}$ and r_{decane} are (0.854±0.086) and (0.951±0.019) nm, respectively. Yang *et al.*[4] considered that the interfacial tension depends on the status of the surfactant molecules adsorbing on the interface, especially the properties of the outermost atoms or groups at the interface region. Therefore, it is concluded that the structure of surfactant at the interface plays an important role in the reducing interfacial tension.

Further, we studied the influence of the *trans*-form dihedral probability on the interfacial tensions. Fig.4 presents the *trans*-form fraction of the dihedral angle (P_{trans}) along the carbon chain of the 4-C16 surfactant molecule. Compared water-NaCl/*n*-alkane with water/*n*-alkane, Fig.4(a, b) shows two obvious changes for the *trans*-form fraction of the dihedral, which associate with dihedral angle 2 (*D*(C2C3C4C5)) and dihedral angle 3 (*D*(C3C4C5C6)). In combination with the interfacial tension change, it is found that the larger the *trans*-form fraction of dihedral angle 3, the lower the interfacial tension in Fig.4(a) and 4(b). In Fig.4(c), the change of the *trans*-form fraction of the dihedral in the water/undecane is very similar to that in the water-NaCl/undecane. For the two systems, the interfacial tensions are close to each other ((31.10±3.31) and (31.08±3.41) mN·m^{-1} for water/undecane and water-NaCl/undecane, respectively). The *trans*-form fraction of the dihedral angle is larger, and the alkyl tail chain is more tilted at the interface. In order to be clearer, the plots of the average dihedral angle (*D*(C3C4C5C6)) of the 4-C16 surfactant *vs* time are shown in Fig.5. Therefore, it is concluded that the change of the interfacial tension is related to the change of dihedral angle 3.

2.3 Radial distribution function

Fig.6 shows the radial distribution functions (RDFs) for the oxygen (O) of the polar head group of surfactant and the oxygen (OW) of water. The O-OW RDFs are similar to each other in both the water/*n*-alkane and water-NaCl/*n*-alkane systems. As shown in Fig.6, the well-pronounced feature is the first sharp peak at (0.267±0.001) nm corresponding to strong hydrogen

Table 3 Alkyl tail length of the *n*-alkane and surfactant

System	r_{nonane}/nm	r_{decane}/nm	$r_{undecane}$/nm	r_{short}/nm	r_{long}/nm	$r_{effective}$/nm
water/nonane	0.859±0.014			0.370±0.018	1.241±0.060	0.871±0.078
water/decane		0.951±0.019		0.372±0.015	1.226±0.071	0.854±0.086
		(0.997±0.103)		(0.384±0.019)	(1.337±0.135)	(0.953±0.136)
water/undecane			1.041±0.023	0.370±0.017	1.231±0.070	0.861±0.087
water-NaCl/nonane	0.859±0.016			0.372±0.013	1.224±0.086	0.852±0.099
water-NaCl/decane		0.952±0.018		0.369±0.019	1.240±0.067	0.871±0.086
water-NaCl/undecane			1.040±0.022	0.371±0.014	1.229±0.084	0.858±0.098

The values in the parentheses are from Ref.[8].

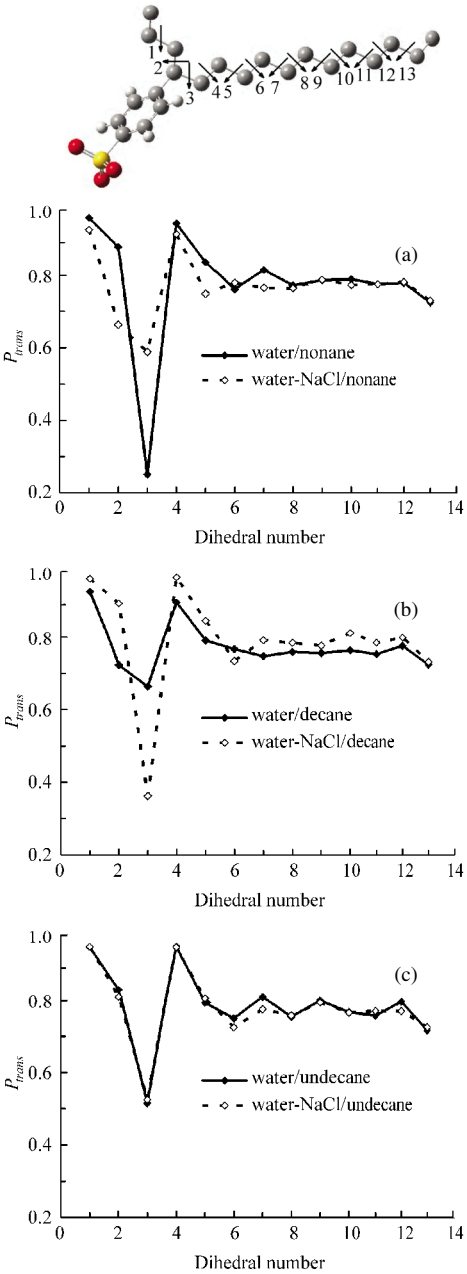

Fig.4 *trans*-form fraction of the dihedral angle along the carbon chain of the 4-C16 surfactant molecule

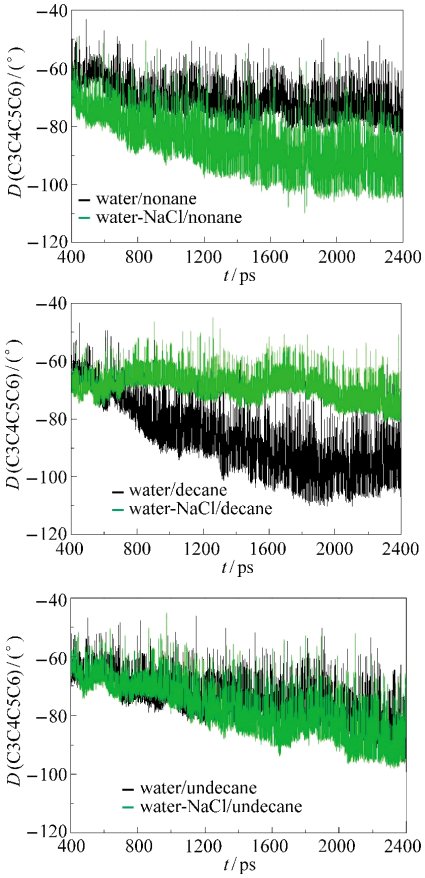

Fig.5 Average dihedral *D*(C3C4C5C6) of the surfactant as a function of simulation time

bonds between the polar head group and water molecules in the O-OW RDFs. Besides, there are the second and third peaks indicating the long-range structures. The second peak occurs at (0.497±0.003) nm. The position difference between the first and second peaks is 0.230 nm, just equal to the length of hydrogen bond. It proves that there are the second-shell water molecules near the polar head group, which form the hydrogen bonds with the first-shell water molecules.

Fig.7 presents the radial distribution function for the oxygen (O) of the polar head group of surfactant and the sodium ion (Na^+). As shown in Figs.6 and 7, the O-Na RDFs are more complicated than the O-OW RDFs. The Na^+ ions are distributed at the interface and in the solution, as the density profiles are described in Fig.3. When NaCl salt is added to the solution, the first peak becomes higher, and the following second, third, and fourth peaks become lower. Among the water(-NaCl)/*n*-alkane,

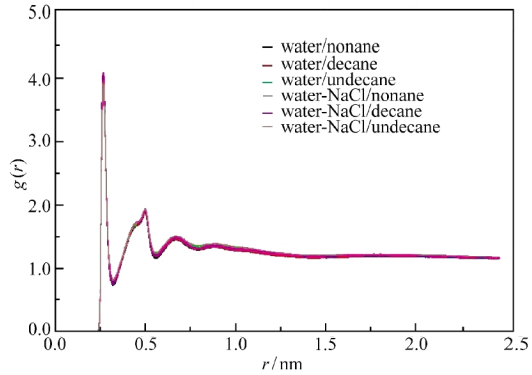

Fig.6 O-OW radial distribution function

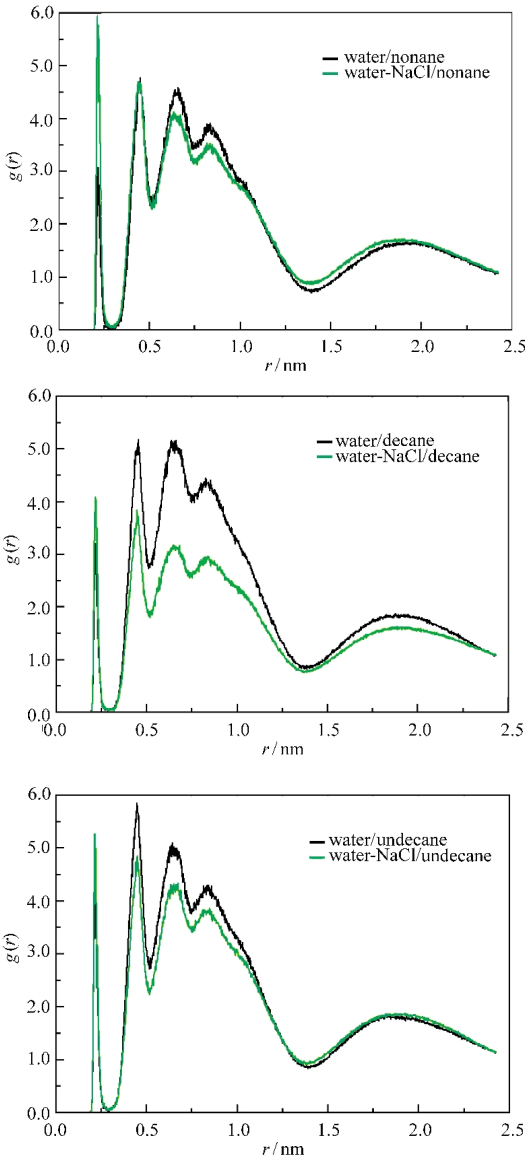

Fig.7 O-Na radial distribution function

the second, third, and fourth peaks in the O-Na RDFs change obviously. The positions of the first two maxima peaks in the O-Na RDFs, which are located at (0.216±0.002) and (0.449±0.003) nm, are different with those in the O-OW RDFs ((0.267±0.001) and (0.497±0.003) nm, respectively). The reason is that the partial charge of Na^+ is larger than one of the hydrogen atoms in water and the interaction between the polar head and Na^+ is stronger than that between the polar head and water. Along with NaCl addition the interaction between the polar head and Na^+ becomes stronger.

3 Conclusions

Using MD simulations, we studied the structures and dynamic properties of anionic surfactants at the water/*n*-alkane (nonane, decane, and undecane) interface. As the same time, we also reported interfacial properties of the systems including the inorganic salt.

The density profiles show that the *n*-alkane and water bulk phases have their own bulk densities, indicating that the system size is fairly large enough to describe the interface between bulk phases. As for the interfacial tension, we found that it was not reasonable to explain as the sample miscibility between surfactant and oil. We observed the relationship between the interfacial tension and the *trans*-form fraction of dihedral angle 3, and found that the larger the *trans*-form fraction of dihedral angle 3, the lower the interfacial tension. The radial distribution functions present that there are the stronger interactions between the polar head group of surfactant with Na^+ and water.

In this paper, we provide much useful information on surfactant at the water/*n*-alkane interface under the different oil phases and the special inorganic salinity conditions, which is helpful in further study on how the surfactants improve the flushing efficiency in the enhanced crude oil recovery.

References

1 Baumgartner, F. N. *Ind. Eng. Chem.*, **1954, 46**: 1349

2 Doe, P. H.; Wade, W. H. *J. Colloid Interface Sci.*, **1977, 59**: 525

3 Doe, P. H.; El-Emary, M.; Wade, W. H. *J. Am. Oil. Chem. Soc.*, **1977, 54**: 570

4 Yang, J.; Qiao, W. H.; Li, Z. S.; Cheng, L. B. *Fuel*, **2005, 84**: 1607

5 (a) Wang, L. Ph. D. Dissertation. Beijing: Graduate University of Chinese Academy of Sciences, 2004 [王 琳. 博士学位论文. 北京: 中国科学院研究生院, 2004]

(b) Gong, Q. T. Ph. D. Dissertation. Beijing: Graduate University of Chinese Academy of Sciences, 2005 [宫清涛. 博士学位论文. 北京: 中国科学院研究生院, 2005]

(c) Jiang, X. M. Ph. D. Dissertation. Beijing: Graduate University of Chinese Academy of Sciences, 2005 [姜小明. 博士学位论文. 北京: 中国科学院研究生院, 2005]

(d) Shi, F. Q. Ph. D. Dissertation. Beijing: Graduate University of Chinese Academy of Sciences, 2005 [史福强. 博士学位论文. 北京: 中国科学院研究生院, 2005]

6 Li, Y.; Zhang, P.; Dong, F. L.; Cao, X. L.; Song, X. W.; Cui, X. H. *J. Colloid Interface Sci.*, **2005, 290**: 275

7 Li, Z. Q.; He, X. J.; Li, Y.; Ma, B. M.; Cao, X. L.; Song, X. W.;

Cui, X. H. *Acta Chimica Sinica*, **2007, 65**: 2803 [李振泉, 何秀娟, 李 英, 马保民, 曹绪龙, 宋新旺, 崔晓红. 化学学报, **2007, 65**: 2803]

8 Jang, S. S.; Lin, S. T.; Maiti, P. K.; Blanco, M.; Goddard III, W. A.; Shuler, P.; Tang, Y. C. *J. Phys. Chem. B*, **2004, 108**: 12130

9 Frisch, M. J.; Trucks, G. W.; Schlegel, H. B.; *et al*. Gaussian 03. Pittsburgh, PA: Gaussian Inc., 2003

10 Martinez, J. M.; Martinez, L. *J. Comput. Chem.*, **2003, 24**: 819

11 Zeng, Z. Q. Organic chemistry. Beijing: Higher Education Press, 1998: 33 [曾昭琼. 有机化学. 北京: 高等教育出版社, 1998: 33]

12 Tsierkezos, N. G.; Molinou, I. E. *J. Chem. Eng. Data*, **1998, 43**: 989

13 van Buuren, A. R.; Marrink, S. J.; Berendsen, J. C. *J. Phys. Chem.*, **1993, 97**: 9206

14 Berendsen, H. J. C.; Postma, J. P. M.; Gunsteren, W. F.; Hermans, J. Intermolecular forces. Reidel: Dordrecht, 1981

15 Schuettelkopf, A. W.; van Aalten, D. M. F. *Acta Cryst. D*, **2004, 60**: 1355

16 Ryckaert, J. P.; Bellemans, A. *Faraday Discuss Chem. Soc.*, **1978, 66**: 95

17 Bekker, H.; Berendsen, H. J. C.; Dijkstra, E. J.; Achterop, S.; van Drunen, R.; van der Spoel, D.; Sijbers, A.; Keegstra, H.; Reitsma, B.; Renardus, M. K. R. Gromacs: a parallel computer for molecular dynamics simulations. //de Groot, R. A.; Nadrchal, J. Eds. Physics computing 92. Singapore: World Scientific, 1993

18 Berendsen, H. J. C.; van der Spoel, D.; van Drunen, R. *Comput. Phys. Commun.*, **1995, 91**: 43

19 Lindahl, E.; Hess, B.; van der Spoel, D. *J. Mol. Mod.*, **2001, 7**: 306

20 van der Spoel, D.; Lindahl, E.; Hess, B.; Groenhof, G.; Mark, A. E.; Berendsen, H. J. C. *J. Comput. Chem.*, **2005, 26**: 1701

21 Hess, B.; Bekker, H.; Berendsen, H. J. C.; Fraaije, J. G. E. M. *J. Comput. Chem.*, **1997, 18**: 1463

22 Nose, S.; Klein, M. L. *J. Chem. Phys.*, **1983, 78**: 6928

23 Nose, S. *J. Chem. Phys.*, **1984, 81**: 511

24 Hoover, W. G. *Phys. Rev. A*, **1985, 31**: 1695

25 Parrinello, M.; Rahman, A. *J. Appl. Phys.*, **1981, 52**: 7182

26 Nosé, S.; Klein, M. L. *Mol. Phys.*, **1983, 50**: 1055

27 Hill, T. L. Introduction to statistical mechanics. New York: Dover, 1986: 314

28 Ono, S.; Kondo, S. Molecular theory of surface tension in liquids// encyclopedia of physics. Flugge, S. Ed. Berlin: Springer, 1960: 134